

# Spinning Gravitating Skym ions

Theodora Ioannidou<sup>a</sup>, Burkhard Kleihaus<sup>by</sup> and Jutta Kunz<sup>bz</sup>

<sup>a</sup> Mathematics Division, School of Technology

Aristotle University of Thessaloniki

Thessaloniki 54124, Greece

<sup>b</sup> Institut für Physik, Universität Oldenburg, Postfach 2503

D-26111 Oldenburg, Germany

March 24, 2022

## Abstract

We investigate self-gravitating rotating solutions in the Einstein-Skym e theory. These solutions are globally regular and asymptotically flat. We present a new kind of solutions with zero baryon number, which possess neither a flat limit nor a static limit.

## 1 Introduction

In non-Abelian field theories coupled to gravity particle-like solutions as well as black holes arise [1]. The latter are of importance as counterexamples to the no-hair conjecture. In recent years, in particular, various stationary rotating non-Abelian black holes have been studied [2]. However, the construction of stationary rotating particle-like solutions is still a difficult task. Although existence of such solutions in non-Abelian gauge field theories has been restricted [3, 4, 5], they can exist in the topologically trivial sector [6, 7]. On the other hand, stationary rotating soliton solutions in flat space have been obtained in the Skym e model [8] and the  $U(1)$  gauged Skym e model [9] in the nontrivial sector.

The Skym e model is a nonlinear chiral field theory in which baryons and nuclei are described in terms of solitons (so-called Skym ions). Due to the long-standing difficulties in finding a satisfactory theoretical model for the interaction of baryons, much effort has been

---

Em ail: ti3@auth.gr

<sup>y</sup>Em ail: kleihaus@theorie.physik.uni-oldenburg.de

<sup>z</sup>Em ail: kunz@theorie.physik.uni-oldenburg.de

devoted to the study of classical and quantised interactions of Skyrme ions. However, the quantization of the Skyrme model is not only difficult since it is a non-renormalizable field theory; but also spinning Skyrme ions must be considered which means that the solutions must consist of massive pions. This follows from the fact that the Skyrme ion can only spin at a frequency up to the pion mass before it begins to radiate pions [10]. Recently in [8], it was shown numerically that a good description of protons and neutrons can be achieved with spinning Skyrme ions, provided the pion mass is chosen twice the experimental value.

The rotating Skyrme ion solutions of [8] are expected to persist, when the coupling to gravity is turned on gradually, analogous to the static Skyrme ion solutions [11]. In the static limit, a branch of gravitating Skyrme ions emerges from the flat space Skyrme ion, when the coupling to gravity is increased from zero [11]. This branch terminates at a maximal value of the coupling parameter, when the coupling to gravity becomes too large for solutions to persist. A second branch of solutions exists which merges with the first one at the maximal value of the coupling parameter and extends back to zero. The solutions on the second branch possess a larger mass and they are unstable [12]. In the limit of vanishing coupling the solutions shrink to zero size and their mass diverges. As shown in [13], in this limit the Skyrme ion solutions approach the lowest mass Bartnik-McKinnon (BM) solution of the SU(2) Einstein-Yang-Mills theory [14].

In this paper we investigate the stationary rotating generalisation of the static gravitating Skyrme ions. We show that in contrast to the static case, additional branches of solutions arise, which are not related to the flat space Skyrme ion or to the BM solution. Most interestingly, we find a new kind of solution with zero baryon number, which exists for arbitrary (finite) coupling parameter, but does not possess a flat space limit. In particular, Section 2 presents the Einstein-Skyrme Lagrangian and the ansatz for the Skyrme field and the metric, which lead to stationary rotating Skyrme ions. In Section 3 the numerical solutions are discussed, while the conclusions are given in Section 4.

## 2 Einstein-Skyrme Theory

The SU(2) Einstein-Skyrme Lagrangian reads

$$\mathcal{L} = \frac{R}{16G} + \frac{1}{4} \text{Tr}(K_\mu^\nu K_\nu^\mu) + \frac{1}{32e^2} \text{Tr}([K_\mu^\nu; K_\nu^\mu][K_\mu^\rho; K_\rho^\mu]) + \frac{m^2}{2} \text{Tr} \frac{U + U^\dagger}{2} \quad (1)$$

and its action is given by

$$S = \int d^4x \sqrt{-g} \mathcal{L} \quad (2)$$

Here  $R$  is the curvature scalar,  $G$  is the Newton constant, and  $e$  are the Skyrme model coupling constants,  $m$  is the pion mass, and  $g$  corresponds to the determinant of the metric. The SU(2) Skyrme field  $U$  enters via  $K_\mu^\nu = \partial_\mu U U^{-1}$ .

Variation of (2) with respect to the metric  $g_{\mu\nu}$  leads to the Einstein equations

$$\begin{aligned} G_{\mu\nu} &= R_{\mu\nu} - \frac{1}{2} g_{\mu\nu} R \\ &= -8\pi G T_{\mu\nu} \quad (3) \end{aligned}$$

where the stress-energy tensor is given by

$$T_{\mu\nu} = -\frac{1}{2} \text{Tr} K_{\mu} K_{\nu} - \frac{1}{2} g_{\mu\nu} K_{\alpha} K^{\alpha} - \frac{1}{8e^2} \text{Tr} g_{\mu\nu} [K^{\alpha}; K^{\beta}][K^{\gamma}; K^{\delta}] + \frac{1}{4} g_{\mu\nu} [K^{\alpha}; K^{\beta}] K^{\gamma} K^{\delta} + g_{\mu\nu} m^2 \text{Tr} \frac{U + U^{\dagger}}{2} \mathbb{1} : \quad (4)$$

For stationary rotating solutions, two commuting Killing vector fields are imposed on the space-time:  $\partial_t$  and  $\partial_{\phi}$  in a system of adapted coordinates  $(t; r; \theta; \phi)$ . In these coordinates the metric can be expressed in Lewis-Papapetrou form

$$ds^2 = -f dt^2 + \frac{m}{f} dr^2 + r^2 d\theta^2 + l r^2 \sin^2 \theta d\phi^2 - \frac{\omega}{r} dt d\phi; \quad (5)$$

where  $f, m, l$  and  $\omega$  are functions of  $r$  and  $\theta$  only.

Then, the total mass and angular momentum are defined by

$$M = \frac{1}{4G} \int_{\Sigma} R_{\mu\nu} k^{\mu} k^{\nu} dV; \quad J = \frac{1}{8G} \int_{\Sigma} R_{\mu\nu} k^{\mu} dV; \quad (6)$$

respectively. Here  $\Sigma$  denotes an asymptotically flat hyper-surface,  $dV$  is the natural volume element on  $\Sigma$ ,  $k^{\mu}$  is normal to  $\Sigma$  and  $k^{\mu} k_{\mu} = 1$ .

In order for finite energy configurations to exist the Skyrme field must tend to a constant matrix at spatial infinity:  $U \rightarrow \mathbb{1}$  as  $|x| \rightarrow \infty$ . This effectively compactifies the three-dimensional Euclidean space into  $S^3$  and implies that the Skyrme fields can be considered as maps from  $S^3$  into  $SU(2)$ . As the third homotopy class of  $SU(N)$  is  $\mathbb{Z}$ , every field configuration is characterized by a topologically invariant integer  $B$ , which can be obtained as

$$B = \int_{\Sigma} B_{\mu\nu} k^{\mu} dV; \quad (7)$$

where  $B_{\mu\nu}$  is the topological current

$$B_{\mu\nu} = \frac{1}{24\pi^2} \text{Tr} (K_{\mu} K_{\nu} K^{\alpha}) : \quad (8)$$

This winding number classifies the solitonic sectors in the model and may be identified with the baryon number of the field configuration.

For spinning Skyrme ion the ansatz is of the form<sup>1</sup>:

$$U = n_1 \mathbb{1} + i n_3 \tau_z + i n_2 (\tau_x \cos(\phi + \omega_s t) + \tau_y \sin(\phi + \omega_s t)); \quad (9)$$

where  $\tau_x, \tau_y, \tau_z$  are the Pauli matrices;  $n_i$  are functions of  $r$  and  $\theta$  only, satisfying the constraint  $C = (1 - n_1^2 - n_2^2 - n_3^2) = 0$ , and the constant  $\omega_s$  corresponds to the spinning frequency of the Skyrme ions.

---

<sup>1</sup>Strictly speaking, the ansatz is neither stationary nor axially symmetric, since it depends explicitly on time and the azimuthal angle. However, the stress-energy tensor does possess the corresponding symmetries. See also Ref. [4].

When deriving the partial differential equations (PDEs) for the Skyrme ion functions  $n_i$ , we have to take into account the constraint  $C = 0$ . This can be achieved by adding the constraint multiplied by some constant, say  $c_0$ , to the Lagrangian and deriving the variational equations:

$$E_i = \partial_r \frac{\partial L}{\partial (\partial_r n_i)} + \partial_\theta \frac{\partial L}{\partial (\partial_\theta n_i)} - \frac{\partial L}{\partial n_i} + 2c_0 n_i = 0 : \quad (10)$$

Then, the constant  $c_0$  can be obtained from the linear superposition  $\sum n_i E_i = 0$ , and substituted back in the PDEs of (10).

### 3 Numerical Solutions

#### 3.1 Parameters and Boundary Conditions

Introducing the dimensionless radial coordinate  $x = r/r_0$ , the gravitational coupling parameter  $\alpha^2 = 4\pi G r_0^2$ , the spinning frequency  $\omega_s = \omega_s/r_0$ , and the pion mass  $m_\pi = m_\pi/r_0$ , action (2) becomes

$$S = \frac{1}{e} \int_0^{\infty} dx \left[ \frac{R}{4} + \frac{1}{4} \text{Tr}(K K^T) + \frac{1}{32} \text{Tr}(K K^T K K^T) + \frac{m_\pi^2}{2} \text{Tr} \frac{U + U^\dagger}{2} \right] 4\pi x^2 dx; \quad (11)$$

while the Einstein equations read:  $G_{\mu\nu} = 2\pi T_{\mu\nu}$ . We also introduce the dimensionless mass  $M = M/r_0$  and angular momentum  $J = J/r_0^2$ . That way, the solutions depend only on the parameters  $\alpha$ ,  $\omega_s$  and  $m_\pi$ . For convenience we will rename  $\omega_s \rightarrow \omega$ .

At the origin, the boundary conditions are

$$n_1(0) = 1; \quad n_2(0) = n_3(0) = 0; \quad \partial_x f_j = 0; \quad \partial_x l_j = 0; \quad \partial_x m_j = 0; \quad \omega(0) = 0; \quad (12)$$

while for large  $x$ , since the asymptotic value of the Skyrme field is the unit matrix and of the metric is the Minkowski metric, we get

$$n_1(\infty) = 1; \quad n_i(\infty)_{i=2,3} = 0; \quad f(\infty) = 1; \quad l(\infty) = 1; \quad m(\infty) = 1; \quad \omega(\infty) = 0; \quad (13)$$

On the  $z$ -axis ( $\theta = 0$ ) the boundary conditions follow from regularity

$$\begin{aligned} \partial_\theta n_1|_{\theta=0} &= 0; \quad n_2(\theta=0) = 0; \quad \partial_\theta n_3|_{\theta=0} = 0; \\ \partial_\theta f|_{\theta=0} &= 0; \quad \partial_\theta l|_{\theta=0} = 0; \quad \partial_\theta m|_{\theta=0} = 0; \quad \partial_\theta \omega|_{\theta=0} = 0; \end{aligned} \quad (14)$$

while in the  $xy$ -plane ( $\theta = \pi/2$ ) from reflection symmetry

$$\begin{aligned} \partial_\theta n_1|_{\theta=\pi/2} &= 0; \quad \partial_\theta n_2|_{\theta=\pi/2} = 0; \quad n_3(\theta=\pi/2) = 0; \\ \partial_\theta f|_{\theta=\pi/2} &= 0; \quad \partial_\theta l|_{\theta=\pi/2} = 0; \quad \partial_\theta m|_{\theta=\pi/2} = 0; \quad \partial_\theta \omega|_{\theta=\pi/2} = 0; \end{aligned} \quad (15)$$

In what follows we will encounter two special cases, the Bartnik-McKinnon solution and the non-trivial solutions in the vacuum sector.

The first, is obtained after re-scaling  $x = \kappa$  and taking the limit of vanishing  $\omega$ . In this limit, the solutions are equivalent to the Bartnik-McKinnon one with lowest mass:

$$n_1 = w(\kappa); \quad n_2 = \frac{q}{1 - n_1^2} \sin \theta; \quad n_3 = \frac{q}{1 - n_1^2} \cos \theta; \quad l = m; \quad \omega = 0; \quad (16)$$

where the gauge potential of the SU(2) Einstein-Yang-Mills theory is parametrized from  $w(\kappa)$  via the relation  $A_i^a = (1 - w(\kappa)) \epsilon_{iaj} \kappa_j = (2\kappa^2)$ .

The second is obtained by setting

$$n_1 = \cos(h); \quad n_2 = \sin(h); \quad n_3 = 0; \quad (17)$$

where the function  $h$  depends on  $x$  and  $\omega$ . Regularity and finite energy of the solutions require that  $h$  vanishes on the  $z$ -axis and at infinity. We will refer to these solutions as 'pion cloud'.

## 3.2 Numerical Results

The solutions are constructed using the software package CADSOL [15] based on the Newton-Raphson algorithm. In order to map the infinite range of the radial variable  $x$  to the finite interval  $[0;1]$  we introduce the compactified radial variable  $x = \kappa/(1 + \kappa)$ . Typical grids contain 70–50 points. The estimated relative errors are approximately 0.1%, except close to  $\kappa_{\max}$  where they become as large as 1%.

In particular, gravitating Skyrmions are constructed and their dependence on the coupling parameter  $\omega$  and the spinning frequency  $\omega_s$  are studied for fixed pion mass:  $m_\pi = 1$ . This sets a limit to the range of the spinning frequency  $\omega_s \leq 1$ . We start the discussion by a qualitative description of the dependence of the solutions on the gravitational parameter  $\omega$  for fixed spinning frequency  $\omega_s$ . Different branches of solutions exist which are characterized by their limit as  $\omega \rightarrow 0$ . First, there are branches of solutions which tend to the flat space Skyrmions and to the scaled BM solution which we call (for obvious reasons) 'Skyrmion' and 'BM' branches, respectively.

Second, branches of solutions exist which form a 'pion cloud' for large  $x$  as  $\omega \rightarrow 0$ . In this limit the solutions resemble a superposition of the 'pion cloud' with either a Skyrmion or the scaled BM solution and are called 'cloudy Skyrmion' and 'cloudy BM' branches, respectively. However, that for the 'cloudy' solutions the limit  $\omega \rightarrow 0$  is singular, as explained below.

For fixed  $\omega_s$  the branches exist up to a maximal value of  $\omega$ , where they merge with a branch of different type. In particular, the way different branches merge depends on the value of  $\omega_s$  relative to the critical value  $\omega_s^{\text{cr}} = 0.9607$ . So, for  $\omega_s < \omega_s^{\text{cr}}$  the 'Skyrmion' branches merge with the 'BM' ones; however for  $\omega_s > \omega_s^{\text{cr}}$ , the 'Skyrmion' and the 'BM' branches merge with the 'cloudy Skyrmion' and the 'cloudy BM' ones, respectively. Moreover, the 'cloudy Skyrmion' branches merge with the 'cloudy BM' branches only when  $\omega_s < \omega_s^{\text{cr}}$ .

Next a quantitative description in terms of the dimensionless mass  $M$  and the value of the function  $l_0 = l(0)$  is presented. Since with vanishing  $\alpha$  the mass diverges on the 'BM', the 'cloudy Skyrmion' and the 'cloudy BM' branches we also consider the scaled masses  $M\alpha$  and  $M\alpha^3$ .

Fig. 1 (a) presents the mass  $M$  for the 'Skyrmion' branches (solid) which merge either with the 'BM' branches (dashed) or the 'cloudy Skyrmion' branches (dotted) when  $\omega_s < \omega_s^{cr}$  and  $\omega_s > \omega_s^{cr}$ , respectively. Note that, as  $\alpha$  increases the mass decreases on the 'Skyrmion' branches, for small  $\alpha$ ; but diverges on the 'BM' and the 'cloudy Skyrmion' branches as  $\alpha$  tends to zero. Also Fig. 1 (a) shows the mass of the 'BM' branches merging with the 'cloudy BM' branches (dash-dotted) when  $\omega_s > \omega_s^{cr}$ ; and the mass of the 'cloudy Skyrmion' branches merging with the 'cloudy BM' branches when  $\omega_s < \omega_s^{cr}$ .

The scaled mass  $M\alpha$  is plotted in Fig. 1 (b). Note that, as  $\alpha$  decreases along the 'BM' branches the scaled mass  $M\alpha$  tends to a finite value which is equal to the mass of the Bartnik-McKinnon solution. Also, Fig. 1 (b) shows the scaled mass  $M\alpha$  of the 'BM' branches as it merges with the 'cloudy BM' branches, and of the 'cloudy Skyrmion' branches as it merges with the 'cloudy BM' branches. Clearly  $M\alpha$  diverges on the 'cloudy Skyrmion' and the 'cloudy BM' branches for vanishing  $\alpha$ .

Fig. 1 (c) reveals that in the limit  $\alpha \rightarrow 0$  the scaled mass  $M\alpha^3$  of the 'cloudy Skyrmion' and the 'cloudy BM' branch tends to a unique value which depends only on  $\omega_s$ .

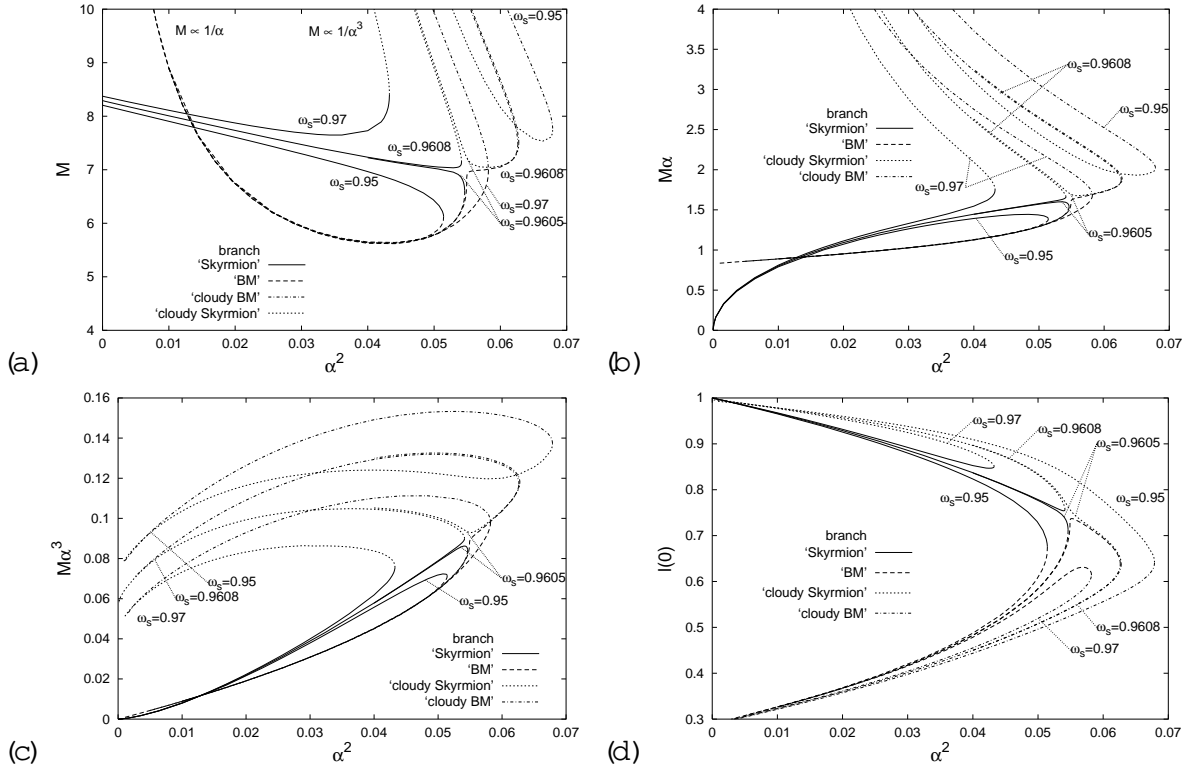


Figure 1: The dimensionless mass  $M$  (a), the scaled masses  $M\alpha$  (b) and  $M\alpha^3$  (c), and the value of  $l$  at the origin (d) as function of  $\alpha^2$  for several values of  $\omega_s$ .

Next we study the quantity  $l_0$  of Fig. 1(d) in order to have a better understanding. Following a solution along a 'Skyrmion' branch which merges with a 'BM' branch,  $l_0$  decreases monotonically first along the 'Skyrmion' branch as  $\alpha$  increases and then along the 'BM' branch as  $\alpha$  decreases, to take the value of the Bartnik-McKinnon solution as  $\alpha \rightarrow 0$ . In contrast, when a 'Skyrmion' branch merges with a 'cloudy Skyrmion' branch,  $l_0$  reaches a minimum on the 'Skyrmion' branch and increases on the 'cloudy Skyrmion' branch as  $\alpha$  decreases. On the other hand, when the 'BM' branch merges with a 'cloudy BM' branch,  $l_0$  increases with increasing  $\alpha$  along the 'BM' branch until it reaches a maximum and decreases with decreasing  $\alpha$  along the 'cloudy BM' branch. Finally, when a 'cloudy Skyrmion' branch merges with a 'cloudy BM' branch,  $l_0$  decreases monotonically if one follows the solutions first on the 'cloudy Skyrmion' branch with decreasing  $\alpha$  and then on the 'cloudy BM' branch with increasing  $\alpha$ .

Also, while we observe that the scaled mass  $M\alpha^3$  of the 'cloudy Skyrmion' and the 'cloudy BM' branches tends to the same value as  $\alpha$  tends to zero (this is not true for the quantity  $l_0$ ). Thus, we conclude that the solutions approach different limits, though with the same (scaled) mass.

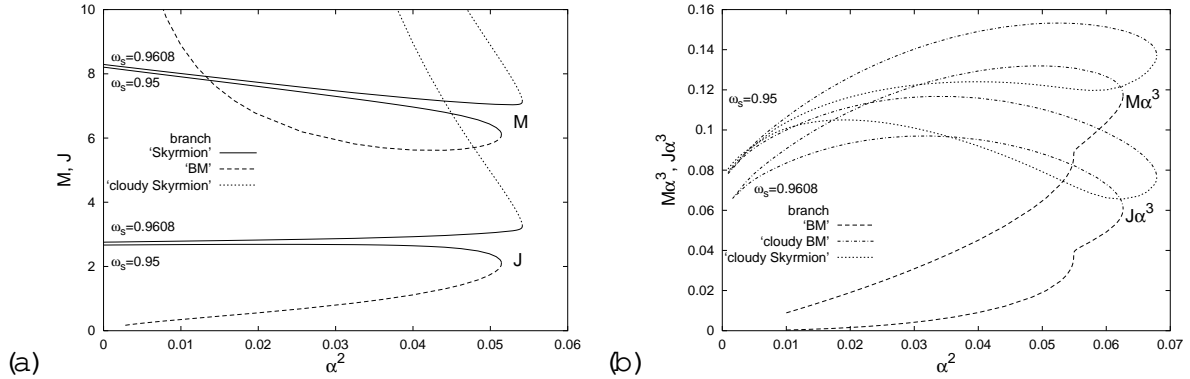


Figure 2: The dimensionless mass  $M$  and angular momentum  $J$  (a), and the scaled mass  $M\alpha^3$  and angular momentum  $J\alpha^3$  (b) as function of  $\alpha^2$  for  $\omega_s = 0.95$  and  $\omega_s = 0.9608$ .

In the following we compare the mass and the angular momentum. We here restrict to  $\omega_s = 0.95 < \omega_s^{cr}$  and  $\omega_s = 0.9608 > \omega_s^{cr}$ , as examples. In particular, Fig. 2(a) shows that when  $\omega_s = 0.95 < \omega_s^{cr}$  the angular momentum decreases monotonically on the 'Skyrmion' branch as  $\alpha$  increases and on the 'BM' branch as  $\alpha$  decreases, while it tends to zero on the 'BM' branch as  $\alpha \rightarrow 0$ . In contrast, for  $\omega_s = 0.9608 > \omega_s^{cr}$  the angular momentum increases monotonically on the 'Skyrmion' branch as  $\alpha$  increases and on the 'cloudy Skyrmion' branch as  $\alpha$  decreases, while in the limit  $\alpha \rightarrow 0$  the angular momentum diverges like  $\alpha^3$ . Fig. 2(b) presents the scaled mass  $M\alpha^3$  and angular momentum  $J\alpha^3$  for the 'BM' and 'cloudy BM' branches when  $\omega_s = 0.9608$  and for the 'cloudy Skyrmion' and 'cloudy BM' branches when  $\omega_s = 0.95$ . As  $\alpha \rightarrow 0$  the (scaled) angular momentum tends to zero on the 'BM' branch, but takes finite values on the 'cloudy' branches.

The new interesting feature of the rotating gravitating Skyrmions is the formation of

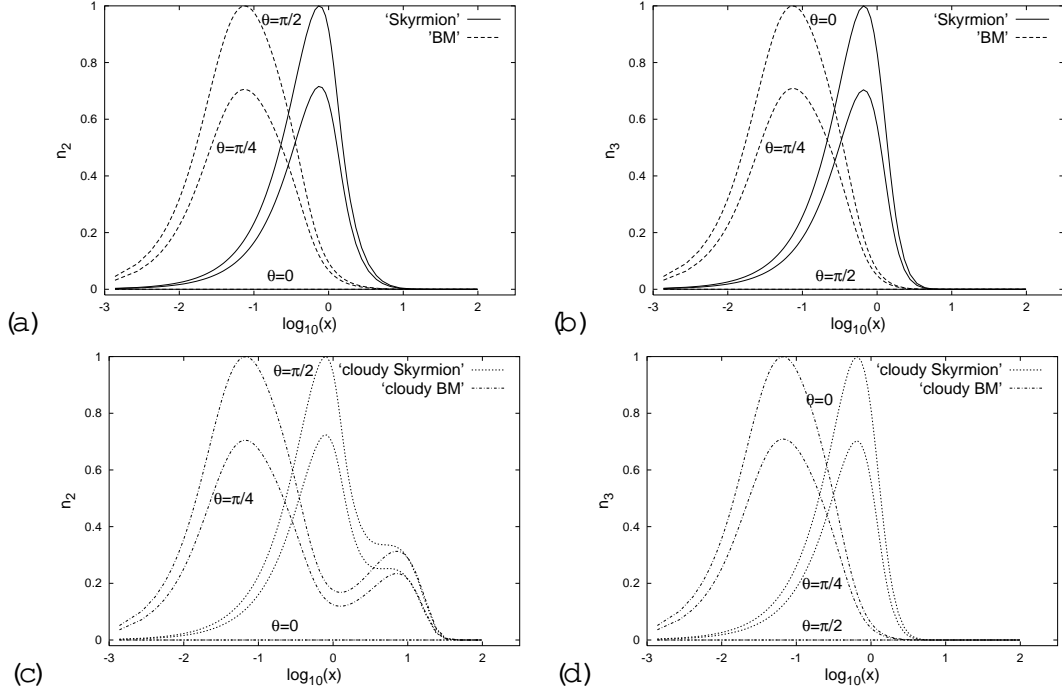


Figure 3: The functions  $n_2$  (left) and  $n_3$  (right) are plotted for  $\theta = 0; \pi/4; \pi/2$  for the four solutions with parameter values  $\beta_s = 0.95$  and  $\beta = 0.1$ .

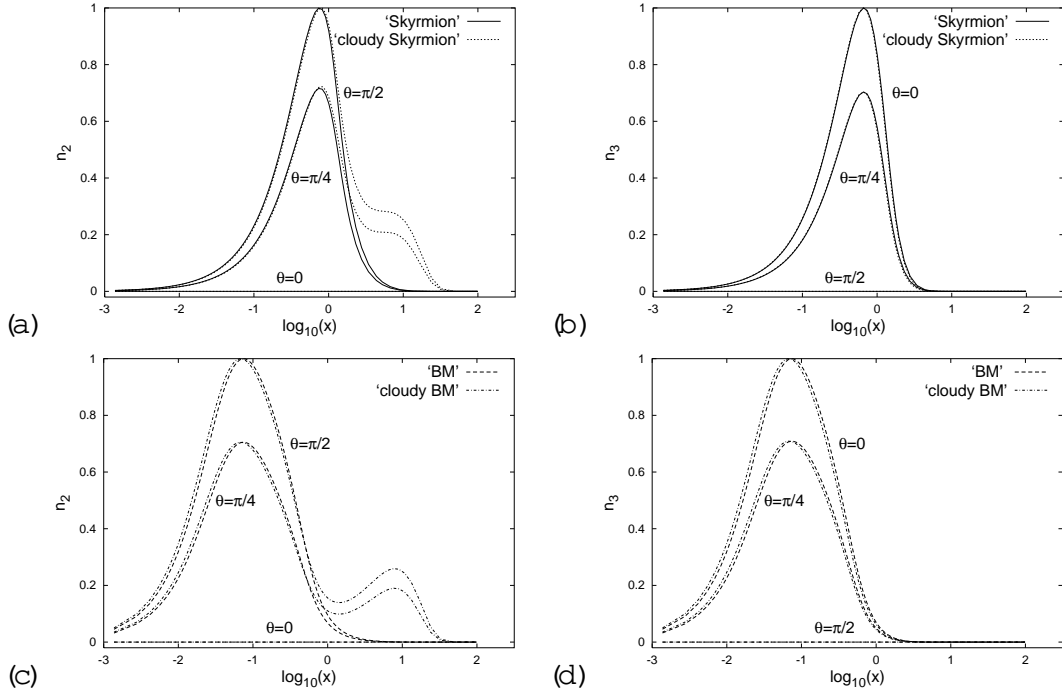


Figure 4: Analogous as Figure 3 for  $\beta_s = 0.9608$ .



the 'pion cloud'. This can be demonstrated by plotting the Skyrme ion functions  $n_2$  and  $n_3$  when  $\alpha = 0.1$  for  $!_s = 0.95 < !_s^{cr}$  and  $!_s = 0.9608 > !_s^{cr}$  as presented in Fig. 3 and Fig. 4 (respectively).

In particular, Figs. 3(a) and (b) show that on the 'Skyrme ion' branch the solution is close to the at space Skyrme ion whereas on the 'BM' branch it is close to the (scaled) Bartnik-McKinnon solution. In contrast, the functions  $n_2$  of the solutions on the 'cloudy Skyrme ion' and 'cloudy BM' branch (presented in Figs. 3(c)) almost coincide at large  $x$  where the 'pion cloud' forms. However, for small  $x$  the functions  $n_2$  are similar in shape to the corresponding ones of Fig. 3(a). Finally, by comparing the functions  $n_3$  of the 'Skyrme ion' and 'BM' solutions (of Fig. 3(b)) with their 'cloudy' counterparts (of Fig. 3(d)) we observe that they are similar in shape for all  $x$  which means that the 'pion cloud' does not reflect itself in the function  $n_2$ .

Fig. 4 presents the solutions on connected branches when  $!_s > !_s^{cr}$ . Note that, the function  $n_2$  of both the 'Skyrme ion' and the 'cloudy Skyrme ion' branch (plotted in Fig. 4(a)) almost coincide for small values of  $x$  and differ for larger  $x$ , where the 'pion cloud' is apparent. In contrast, the functions  $n_3$  are almost identical for both solutions as shown in Fig. 4(b). Similar observations hold for the solutions of the 'BM' branch and the 'cloudy BM' branch plotted in Fig. 4(c)-(d).

On the 'cloudy BM' branch the scaled BM solution in the core separates from the surrounding 'pion cloud' as  $\alpha$  decreases. Therefore, in what follows, we show that pure 'pion cloud' solutions can be constructed numerically by extracting the data of the 'pion cloud'. The ansatz for the 'pion cloud' solution is given by

$$U = \cos(h)\mathbb{1} + i\sin(h)(\cos(' + !_s t)_x + \sin(' + !_s t)_y); \quad (18)$$

where the boundary conditions for the profile function  $h(x; \alpha)$  follow from finite mass and regularity requirements and read as

$$h(0; \alpha) = 0; \quad h(1; \alpha) = 0; \quad h(x; \alpha = 0) = 0; \quad @ h(x; \alpha = \infty) = 0; \quad (19)$$

For these solutions  $n_3 = 0$  so the chiral matrix can be regarded as a map from  $S^3 \rightarrow S^2$  and thus, the 'pion cloud' solutions have zero baryon number. In addition, due to the boundary conditions of the profile function  $h(x; \alpha)$ , the 'pion cloud' solutions can be deformed continuously to the vacuum.

Fig. 5 presents the scaled mass  $M^{-3}$  of the 'pion cloud' solutions and of the Skyrme ions on the 'cloudy' branches as function of  $\alpha^2$  for fixed  $!_s = 0.95$ . Note that, for small  $\alpha$  the masses of the 'cloudy Skyrme ion' and 'cloudy BM' solutions coincide with the mass of the 'pion cloud' solution. However, whereas the branches of the Skyrme ion solutions exist only up to a maximal value of  $\alpha$ , the 'pion cloud' solutions exist for arbitrarily large  $\alpha$ .

Indeed, as  $\alpha$  increases the magnitude of  $h$  decreases linearly like  $1/\alpha$ . So by expanding the Lagrangian up to quadratic order in  $h$  yields

$$L_h = \frac{R}{2} \frac{1}{\alpha^2} @_x h @_x h + \frac{1}{2} @ h @ h + \frac{f}{4x^2 \sin^2} h^2 - \frac{1}{f} !_s \frac{!}{x} h^2 + m^2 h^2; \quad (20)$$

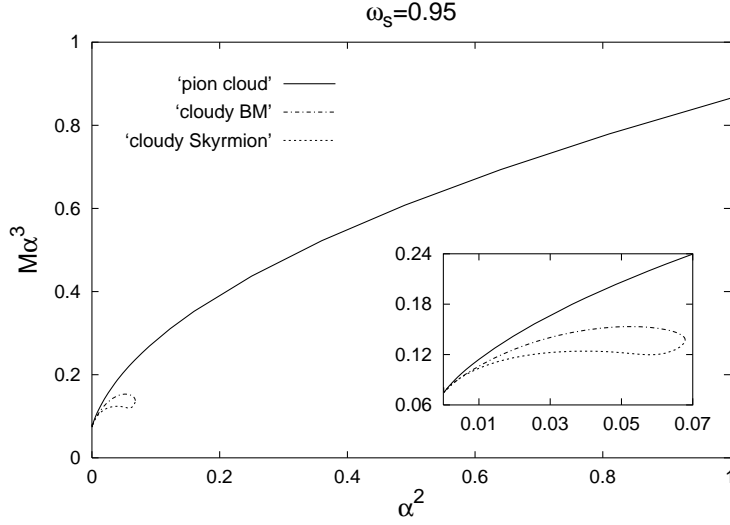


Figure 5: The scaled mass  $M\alpha^3$  for the ‘pion cloud’ solutions and the Skyrmion solutions on the ‘cloudy Skyrmion’ and the ‘cloudy BM’ branches for  $\omega_s = 0.95$ .

which is equivalent to the Lagrangian of the rotating boson star

$$L_{BS} = \frac{R}{2} \int d^3x \left( \frac{1}{2} \dot{\phi}^2 - \frac{1}{4} g^2 (\phi^2 - 1)^2 - V(\phi) \right) \quad (21)$$

for  $\phi = h(x; t) e^{i(\theta - \omega_s t)}$  and  $V(\phi) = \frac{1}{2} \phi^2 m^2 = 2$ . The limit  $\omega_s \rightarrow 1$  of rotating boson stars has been studied in Ref. [16] (though with different notation) where it was shown that the field equations become independent of the coupling parameter after re-scaling  $h = \hat{h}$ . Moreover, it was argued in [16] that several branches of solutions exist in certain ranges of  $\omega_s$  which suggests that several branches of ‘pion cloud’ solutions might (also) exist, at least for large values of  $\omega_s$ .

In the limit  $\omega_s \rightarrow 0$  the scaled mass  $M\alpha^3$  takes finite values. By introducing the scaled radial coordinate  $\rho = \alpha x$ , the Skyrme field equations reduces to the constraint

$$\sin^2(h) \cos(h) \omega_s^2 - f m^2 = 0; \quad (22)$$

as  $\omega_s \rightarrow 0$ . This implies that the Skyrme field function is either  $h = 0$  or  $\cos(h) = f m^2 / \omega_s^2$ . Note that none of these solutions can hold globally; the former one yields the trivial solution and the latter is not consistent with the asymptotic boundary conditions  $h \rightarrow 0$  and  $f \rightarrow 1$  for  $\omega_s^2 < m^2$ . However, both can hold locally. Indeed, we find the solution

$$\begin{aligned} \cos(h) &= f \frac{m^2}{\omega_s^2}; & f > g^2 D = (0; 0] & \quad (0; \infty) \\ h &= 0; & \text{elsewhere;} \end{aligned}$$

where  $0$  depends on  $\omega_s$ . Although this solution for  $h$  is not continuous at the origin and on the  $z$ -axis, the metric functions are continuous globally. Moreover, in the domain  $D$  the

function  $h$  depends only on the radial coordinate  $\rho$ . Consequently, the metric is spherically symmetric and, for  $\rho \rightarrow 0$ , given by the Schwarzschild solution.

Thus, in the limit  $\Omega \rightarrow 0$  the 'pion cloud' becomes confined to the finite domain  $D$ . Outside of  $D$  the metric is the vacuum solution determined by the connecting conditions at  $\rho_0$ . To see the physical picture, however, we have to return to unscaled coordinates. Then the domain  $D$  extends over the whole space, except the  $z$ -axis and infinity. Consequently, the 'pion cloud' occupies an increasing volume in space as  $\Omega$  decreases.

The profile function  $h$  is plotted in Fig. 6(a) as function of the cylindrical coordinates  $\rho = x \sin \theta$ ,  $z = x \cos \theta$  for  $\Omega_s = 0.95$  and  $\Omega = 0.07$  and in Fig. 6(b) as function of the scaled coordinates  $\rho^0 = \rho \sin \theta$ ,  $z^0 = z \cos \theta$  for such parameter values that the constraint is almost satisfied (ie.  $\Omega_s = 0.95$  and  $\Omega = 10^{-4}$ ).

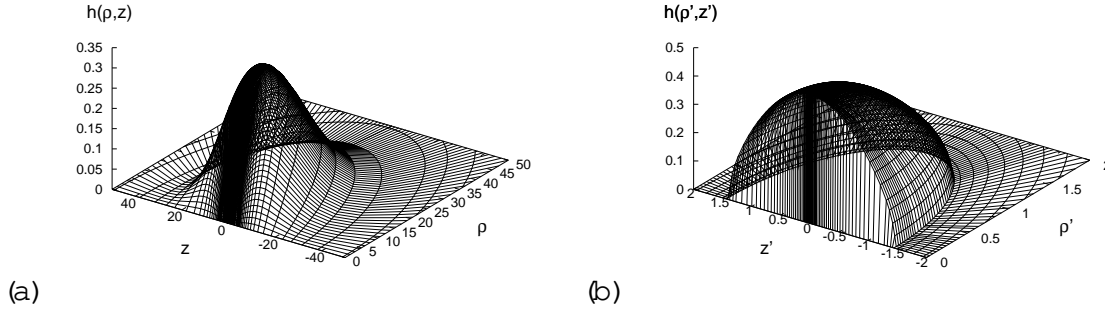


Figure 6: (a) The 'pion cloud' profile function  $h(\rho, z)$  when  $\Omega_s = 0.95$  and  $\Omega = 0.07$ . (b) Same as (a) for  $\Omega = 10^{-4}$  in scaled coordinates  $\rho^0 = \rho \sin \theta$ ,  $z^0 = z \cos \theta$ .

Finally we state that the 'pion cloud' solutions do not exist for arbitrarily small  $\Omega_s$ . In fact, we observed that the coefficient of the second order derivative term in the Skyrme field equation

$$f^2 \sin^2(\theta) \left( \Omega_s^2 - \frac{1}{r^2} \right) \sin^2(\theta) - f^2 r^2 \sin^2(\theta) \left( \partial_{rr}^2 h + \frac{1}{r^2} \partial_{\theta\theta}^2 h + \dots \right) = 0 \quad (23)$$

develops a zero at some point on the  $\theta = \pi/2$  axis, when  $\Omega_s$  decreases to a critical value, and no solution exists for  $\Omega_s$  below the critical value. Therefore, the 'pion cloud' solutions do not possess a static limit.

## 4 Conclusions

We studied stationary rotating solutions of the Einstein-Skyrme theory. These solutions are asymptotically flat, globally regular and axially symmetric. Branches of stationary rotating Skyrmions emerge from corresponding branches of static Skyrmions, when the rotational frequency is increased from zero. If the rotational parameter  $\Omega_s$  is smaller than

a critical value, the rotating Skyrme ions on these branches behave similar to their static counterparts, when the coupling to gravity is varied. However, additional branches of solutions exist, which do not have a flat space limit. These branches are characterised by the formation of a 'pion cloud' for small values of the coupling  $\beta$ .

In addition to the rotating Skyrme ions with baryon number one, we found new solutions in the topologically trivial sector. These 'pion cloud' solutions are also asymptotically flat and globally regular, but possess neither a flat limit nor a static limit. In contrast to the Skyrme ions the 'pion cloud' solutions exist for arbitrary coupling, i.e.  $0 < \beta < 1$ .

Axially symmetric rotating Skyrme ions with higher baryon number  $B > 1$  should easily be obtained by the replacement  $\beta \rightarrow B\beta$  in the ansatz Eq. (9).

Einstein-Skyrme theory also possesses black hole solutions. So far the Skyrme ion black holes have been studied in the static limit only. Families of black hole solutions emerge from the globally static regular Skyrme ions, when the horizon radius is increased from zero. Similarly, we expect several families of stationary rotating Skyrme ion black holes to emerge from the globally regular rotating Skyrme ions on the different branches obtained here [17]. Moreover, one may speculate that also stationary rotating black holes emerge from the 'pion cloud' solutions.

Acknowledgment

BK gratefully acknowledges support by the DFG under contract KU 612/9-1 and TI thanks Oldenburg University for its hospitality.

## References

- [1] for an overview see e.g. M. S. Volkov and D. V. Gal'tsov, Phys. Rept. 319, 1 (1999).
- [2] M. S. Volkov and N. Straumann, Phys. Rev. Lett. 79 (1997) 1428;  
O. Brodbeck, M. Heusler, N. Straumann and M. S. Volkov, Phys. Rev. Lett. 79 (1997) 4310;  
B. Kleihaus and J. Kunz, Phys. Rev. Lett. 86 (2001) 3704;  
B. Kleihaus, J. Kunz and F. Navarro-Lerida, Phys. Lett. B 599 (2004) 294;  
B. Kleihaus, J. Kunz and F. Navarro-Lerida, Phys. Rev. D 69 (2004) 064028;  
B. Kleihaus, J. Kunz and F. Navarro-Lerida, Phys. Rev. Lett. 90 (2003) 171101.
- [3] J. J. Van der Bij and E. Radu, Int. J. Mod. Phys. A 17 (2002) 1477.
- [4] M. S. Volkov and E. W. Ohnert, Phys. Rev. D 67 (2003) 105006.
- [5] J. J. Van der Bij and E. Radu, Int. J. Mod. Phys. A 18 (2003) 2379.
- [6] V. Paturyan, E. Radu and D. H. Tchrakian, Phys. Lett. B 609 (2005) 360.
- [7] B. Kleihaus, J. Kunz and U. N. Neemann, Phys. Lett. B 623 (2005) 171.
- [8] R. A. Battye, S. Kusch and P. M. Sutcliffe, Phys. Lett. B 626 (2005) 120.

- [9] E. Radu and D. H. Tchrakian, *Phys. Lett. B* 632 (2006) 109
- [10] E. Braaten and J. P. Ralston, *Phys. Rev. D* 31 (1985) 598;  
M. Bander and F. Hayot, *Phys. Rev. D* 30 (1984) 1837;  
K. F. Liu and J. S. Zhang, *Phys. Rev. D* 30 (1984) 2015.
- [11] H. Luckock and I. Moss, *Phys. Lett. B* 176 (1986) 341;  
H. Luckock, Black hole skyrmions, *Proceedings of the 1986 Paris-Meudon Colloquium*,  
eds. H. J. de Vega, and N. Sanchez, (World Scientific, Singapore, 1987);  
S. Droz, M. Heusler and N. Straumann, *Phys. Lett. B* 268 (1991) 371.
- [12] M. Heusler, S. Droz and N. Straumann, *Phys. Lett. B* 271 (1991) 61.
- [13] P. Bizon and T. Chmaj, *Phys. Lett. B* 297 (1992) 55.
- [14] R. Bartnik and J. McKinnon, *Phys. Rev. Lett.* 61 (1988) 141.
- [15] W. Schonauer and R. Wei, *J. Comput. Appl. Math* 27 (1989) 279;  
M. Schauder, R. Wei and W. Schonauer, *The CADSO L Program Package*, Universitat  
Karlsruhe, Interner Bericht Nr. 46/92 (1992).
- [16] B. Kleihaus, J. Kunz and M. List, *Phys. Rev. D* 72 (2005) 064002.
- [17] T. Ioannidou, B. Kleihaus and J. Kunz, in preparation.